

# Progress toward controlling *in vivo* fibrillating sheep atria using a nonlinear-dynamics-based closed-loop feedback method

Daniel J. Gauthier

*Department of Physics and Department of Biomedical Engineering, Duke University and Center for Nonlinear and Complex Systems, Box 90305, Durham, North Carolina 27708*

G. Martin Hall

*Department of Physics, Duke University and Center for Nonlinear and Complex Systems, Box 90305, Durham, North Carolina 27708*

Robert A. Oliver, Ellen G. Dixon-Tulloch, and Patrick D. Wolf

*Department of Biomedical Engineering, Duke University and Center for Nonlinear and Complex Systems, Box 90305, Durham, North Carolina 27708*

Sonya Bahar

*Department of Physics, Duke University and Center for Nonlinear and Complex Systems, Box 90305, Durham, North Carolina 27708*

(Received 25 February 2002; accepted 23 May 2002; published 23 August 2002)

We describe preliminary experiments on controlling *in vivo* atrial fibrillation using a closed-loop feedback protocol that measures the dynamics of the right atrium at a single spatial location and applies control perturbations at a single spatial location. This study allows investigation of control of cardiac dynamics in a preparation that is physiologically close to an *in vivo* human heart. The spatial-temporal response of the fibrillating sheep atrium is measured using a multi-channel electronic recording system to assess the control effectiveness. In an attempt to suppress fibrillation, we implement a scheme that paces occasionally the cardiac muscle with small shocks. When successful, the inter-activation time interval is the same and electrical stimuli are only applied when the controller senses that the dynamics are beginning to depart from the desired periodic rhythm. The shock timing is adjusted in real time using a control algorithm that attempts to synchronize the most recently measured inter-activation interval with the previous interval by inducing an activation at a time projected by the algorithm. The scheme is “single-sided” in that it can only shorten the inter-activation time but not lengthen it. Using probability distributions of the inter-activation time intervals, we find that the feedback protocol is not effective in regularizing the dynamics. One possible reason for the less-than-successful results is that the controller often attempts to stimulate the tissue while it is still in the refractory state and hence it does not induce an activation. © 2002 American Institute of Physics. [DOI: 10.1063/1.1494155]

**In this article, we investigate a scheme for controlling the dynamics of a sheep heart during atrial fibrillation. It is desirable to devise such schemes because human atrial fibrillation can lead to a reduced quality of life and repeated hospitalizations. The experiments on sheep hearts serve as a model for human atrial fibrillation and hence successful control of *in vivo* sheep heart dynamics is the first step toward the development of an internal defibrillator for humans. The method is based on techniques developed by the nonlinear dynamics community for controlling chaos. It uses real-time measurements of the time interval between electrical depolarizations of the muscle at a single location on the heart to determine the time at which a small shock is applied to the tissue in an attempt to regularize the electrical depolarizations. The experiment is conducted with the chest open and a fine grid of electrodes placed on the outer surface of the heart to measure the electrical depolarizations as a function of time at numerous spatial locations to determine the effectiveness of control. We describe previous research on controlling cardiac dynamics using small shocks, our experi-**

**mental methods, and our observations. We find that our control protocol is not effective in controlling the sheep heart dynamics in these preliminary experiments, and we suggest possible ways to improve the technique. Hence, this article serves as a progress report to stimulate future research.**

## I. INTRODUCTION

The heart is a complex nonlinear system designed to pump blood effectively. Its mechanical contractions are mediated by waves of electrochemical excitation that propagate through the heart. These waves of excitation are followed by a refractory period when the tissue cannot respond to further stimulation, a fundamental characteristic of the generic, idealized dynamical system classified as an “excitable media.”

In a healthy heart, the waves of excitation cause a coordinated contraction of the muscle starting near the top of the right atrium at the sino-atrial node, progressing to the ventricles through the atrioventricular node and the Purkinje fi-

bers, and terminating near the base of the heart. This type of behavior is known as normal sinus rhythm. In some situations, even in a nominally healthy heart, this orderly procession of waves can evolve into a complex dynamical state known as fibrillation in which the heart rate is elevated and the muscle contractions are uncoordinated.<sup>1,2</sup> Fibrillation in the atria is usually not life-threatening, but can lead to an increased risk of stroke and often leaves a person feeling tired or having a lack of energy. Ventricular fibrillation, however, results in a rapid loss of blood pressure, leading to death within a few minutes if left untreated. The most common strategy for terminating ventricular fibrillation is to apply a large electric shock designed to stop temporarily all cardiac activity, with the hope that a normal rhythm will start with the next heart beat.<sup>3-5</sup> Such a strategy alters significantly the dynamical state of the heart, is not always successful, and is painful to the patient.

Another possible approach to this problem is to administer occasional, small electrical stimuli to the heart muscle, where the strength and timing of the shocks are based on a nonlinear dynamics closed-loop feedback control algorithm. This approach is suggested by recent research on nonlinear dynamical systems displaying temporal instabilities and chaos, where it is now possible to control chaos, delay the onset of bifurcations and instabilities, and direct a trajectory to a desired target state by applying only minute perturbations to the system. The control strategies are quite general and do not require a detailed mathematical model of the system. The key idea is to design perturbations that direct the system near to or stabilize it about one of the unstable periodic orbits embedded in the system.<sup>6-8</sup> Motivated by successes in applying these methods to a variety of physical systems, recent attention has focused on controlling biological systems such as the heart.<sup>9-13</sup> For example, Hall and Gauthier<sup>14</sup> have recently suppressed alternans (a period-2 response pattern) in small pieces of paced cardiac muscle using an approach similar to that described in this paper.

Several hurdles have to be overcome before this approach can be applied successfully to a whole fibrillating heart. One primary issue is that the heart displays complex behavior as a function of time *and* space,<sup>15,16</sup> which may be a manifestation of the deterministic behavior known as *spatio-temporal chaos*.<sup>17</sup> It is not clear whether the chaos control algorithms, designed originally for suppressing *temporal* instabilities, can be applied to fibrillation. Controlling spatio-temporal complexity using small perturbations is interesting from a fundamental nonlinear dynamics perspective because it is not yet firmly established whether a generic system can be characterized by unstable period orbits, and no general control algorithms have been established. One suggested approach is to place standard chaos controllers designed to suppress temporal instabilities at a few or many spatial locations.<sup>18</sup> A recent study suggests that it may be possible to stabilize *in vivo* human atrial fibrillation by applying control at a single spatial location.<sup>19</sup>

The primary purpose of this paper is to describe preliminary experiments on controlling *in vivo* fibrillating sheep atria using a closed-loop feedback protocol in combination with a high-density mapping system to access the size of the

spatial region of the heart that is captured by the small shocks. Our hypothesis is that control should be possible over a finite spatial region around the control point. For our specific protocol, we find that the shocks have little effect on the dynamics. This observation may be due to the possibility that the shocks are delivered when the tissue located in the vicinity of the stimulus electrode is in the refractory (unexcitable) state. However, one experimental trial (out of a total of 80 in 2 animals) showed that the protocol resulted in a noticeable decrease in local activation rate [see Fig. 8(E)]. Future research is needed to determine whether the rate of successful control is limited by our choice of a control protocol or because the spatio-temporal dynamics cannot be effected by a controller placed at a single spatial location.

In the next section of the paper, we review related research on controlling cardiac dynamics using small shocks. In Sec. III, we describe the experimental setup for measuring the spatio-temporal dynamics of the heart and give examples of the observed behaviors in Sec. IV. We go on in Sec. V to describe the nonlinear-dynamics-based feedback controller, describe our results in Sec. VI, and discuss our findings in Sec. VII.

## II. CONTROLLING CARDIAC DYNAMICS USING SMALL SHOCKS

The idea that small electrical stimuli can affect the dynamics of the heart is not new. It is well known that arrhythmias such as atrial flutter and ventricular tachycardia can be initiated and terminated by one or more properly timed stimuli.<sup>20</sup> Unfortunately, attempts to interrupt atrial or ventricular fibrillation have been less successful. Allesie *et al.*<sup>21</sup> have successfully entrained the dynamics of a spatially localized portion of the myocardium during atrial fibrillation using rapid pacing. This procedure did not result in defibrillation, however: complex dynamics reappeared after the pacing was terminated. Similarly, KenKnight *et al.*<sup>22</sup> captured the local dynamics during ventricular fibrillation and also did not achieve defibrillation.

Approaching the problem from a different perspective, Garfinkel *et al.*<sup>9</sup> have demonstrated that it is possible to stabilize cardiac arrhythmias in an *in vitro* heavily medicated small piece of the intraventricular septum of a rabbit heart by administering small, occasional electrical stimuli. The protocol is referred to as proportional perturbation feedback (PPF). In terms of the behavior of the heart, the scheme uses feedback to stabilize periodic beating (the unstable dynamical state) and destabilize complex rhythms using small perturbations. Crucial to this strategy is the concept that the heart can display two different dynamical behaviors under essentially identical physiological conditions, such as normal sinus rhythm and fibrillation or tachycardia and fibrillation, for example. In the PPF method, the dynamics are controlled by placing the state of the system onto the stable manifold of the desired unstable periodic orbit (rather than moving the location of the stable manifold as used in the original proposal for controlling chaotic behavior<sup>6-8</sup>). Note that variations of this method for controlling cardiac dynamics have been suggested,<sup>23</sup> some of which are simpler and more robust.<sup>24,25</sup> The PPF control strategy has also been used by

Schiff *et al.*<sup>26</sup> to stabilize the electrical behavior of the rat hippocampus, suggesting that it may be possible to develop an intervention protocol for epilepsy.

While these results are intriguing, they are surrounded by some controversy because of the claim that chaos exists in the heart and brain based on the detection of unstable period orbits in the system. In an attempt to clarify this situation, Pierson and Moss<sup>27</sup> investigated the influence of noise on the analysis procedure and find that it is indeed capable of detecting unstable periodic orbits even in the presence of large amounts of noise. On the other hand, Christini and Collins<sup>28</sup> have suggested that PPF can be used even in situations where the dynamics are driven by stochastic, rather than deterministic, influences.

In parallel to the research on controlling the dynamics of complex systems, some research has focused on cardiac arrhythmias that are well-characterized by a low-dimension mathematical description and hence should be amenable to control. Taking this approach, Hall *et al.*<sup>10</sup> demonstrated that an adaptive controller can suppress atrio-ventricular nodal conduction alternans in an *in vitro* rabbit heart model, and Christini *et al.*<sup>12</sup> successfully applied the same method in an *in vivo* human heart model. This arrhythmia occurs when electrical signals from the atria pass through the atrio-ventricular node (essentially a one-dimensional conduction pathway) into the ventricles and back to the atria via an abnormal conduction pathway. The control protocol used to suppress alternans in their experiments is based on a comparison of the most recently observed interbeat interval with the previous interval. This method has been analyzed by Gauthier and Socolar<sup>29</sup> and Hall and Christini,<sup>30</sup> and is similar to the one used to control the dynamics of physical systems.<sup>31</sup> More recently, Hall and Gauthier have used a variation of this technique to suppress alternans in small pieces of bullfrog cardiac muscle where spatial-temporal instabilities cannot occur.<sup>14</sup>

While these results suggest that nonlinear-dynamics-based methods can be applied to the heart, they demonstrate only that *temporal* complexity of a dynamical system can be controlled. There is not yet a general approach to controlling systems that display *spatio-temporal* complexity such as that displayed by the heart during fibrillation.<sup>1,2,15,16</sup> Toward this goal, Glass and Josephson<sup>32</sup> established criteria for resetting and annihilation of reentrant arrhythmias; Biktashev and Holden<sup>33</sup> demonstrated that proportional feedback control can induce drift of spiral waves in a model of cardiac muscle; Aranson *et al.*<sup>34</sup> showed that external stimuli can stabilize meandering spiral waves; Osipov *et al.*<sup>35</sup> demonstrated that the introduction of specific forms of tissue inhomogeneity can lead to suppression of spiral waves; Osipov and Collins<sup>36</sup> found that uniform excitation of the tissue or excitation at the leading edge of a wave can lead to termination of the wave; Watanabe and Gilmour<sup>23</sup> proposed a strategy that uses small stimuli to prevent cardiac rhythm disturbances; Rappel *et al.*<sup>18</sup> showed that the break up of spiral wave patterns can be suppressed by applying electrical stimuli at many spatial locations; and Sinha *et al.*<sup>37</sup> demonstrated that spiral wave patterns can be terminated by pacing tissue using a two-dimensional grid of electrodes.

There are several issues that must be addressed before these recent results can be put to practice. In the works of Biktashev and Holden, Osipov and Collins, Watanabe and Gilmour, Rappel *et al.*, and Sinha *et al.*, the use of spatially uniform forcing function or application of perturbations at numerous spatial locations is assumed, a requirement that is not possible with current technology. Also, the results of Aranson *et al.* and Glass and Josephson were obtained using a simplified model of cardiac dynamics whose properties are, in many aspects, different from the properties of cardiac muscle. Finally, it is not clear how tissue inhomogeneities of the form required by Osipov *et al.* can be introduced in an intact heart.

On the other hand, preliminary research by Ditto and collaborators<sup>19</sup> suggests that it is possible to capture at least a portion of a fibrillating human atrium using the PPF method, where the heart dynamics are recorded and control stimuli are delivered through a quadrupolar electrode catheter inserted into the right atrium. It was observed that the wide variation of the inter-beat intervals could be suppressed using their control technique. However, due to the limited number of sensors, it could not be determined what fraction of the entire atrium was controlled. In addition, atrial fibrillation was terminated only rarely using this method. Experiments using many sensors at different spatial locations are needed to determine whether the methods used in the preliminary work of Ditto and collaborators can successfully capture the entire atrium.

The purpose of our study is to attempt to control *in vivo* sheep atrial fibrillation using a feedback controller that measures the dynamics of the atria and applies control perturbations at a single spatial location. This study allows investigation of control of cardiac dynamics in a preparation that is physiologically close to an *in vivo* human heart. Both the temporal and spatial response of the fibrillating sheep atria are measured using a multi-channel electronic recording system.<sup>38</sup> To suppress fibrillation, we implement a control scheme that does not require *a priori* knowledge of the state of the tissue to be stabilized similar to the technique used by Hall *et al.*,<sup>10</sup> Christini *et al.*,<sup>12</sup> and Hall and Gauthier.<sup>14</sup> This controller attempts to stabilize an unstable period-one behavior embedded in the fibrillation that may or may not be the normal sinus rhythm.

### III. EXPERIMENTAL METHODS AND PREPARATION

The experimental model is an *in vivo* sheep atria preparation that allows the investigation of fibrillation in a preparation that is similar to a human heart. We use the atria because the animal can sustain atrial fibrillation for an extended period of time, whereas ventricular fibrillation is fatal within few minutes and hence the animal must be rescued frequently using large defibrillation shocks.

In our experiments, all methods are in accordance with a protocol approved by the Duke University Institutional Animal Care and Use Committee and conform to the Research Animal Use Guidelines of the American Heart Association. After recording the heart rate the sheep is anesthetized with ketamine hydrochloride (15–22 mg/kg IM). Once anesthesia

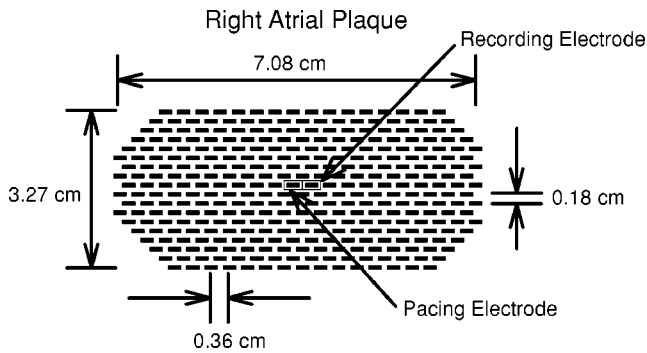


FIG. 1. Layout of the electrodes in the cardiac mapping plaque. The area per electrode is  $0.06 \text{ cm}^2$ .

is achieved, the animal is intubated with a cuffed endotracheal tube and ventilated with a North American Drager mode SAV ventilator. Isoflurane gas (1%–5%) is administered continuously to maintain adequate anesthesia. An orogastric tube is passed into the stomach to prevent rumen aspiration. Femoral arterial blood pressure and the Lead II electrocardiogram (ECG) are continuously displayed and monitored. Blood is withdrawn every 30–60 min to determine  $p\text{H}$ ,  $p\text{O}_2$ ,  $p\text{CO}_2$ , total  $\text{CO}_2$ , base excess and the concentrations of  $\text{Ca}^{2+}$ ,  $\text{K}^+$ ,  $\text{Na}^+$ , and  $\text{HCO}_3^-$ . Normal physiological levels of the above are maintained by adjusting the ventilator and by intravenous injection of electrolytes. A Ventritex defibrillator (Sunnyvale, CA, Model HV02000) is used to terminate inadvertently induced ventricular fibrillation by placing the defibrillator paddles directly on the surface of the heart and applying a large shock.

The spatio-temporal dynamics of the atria are measured using a multi-channel electronic mapping system developed by Wolf *et al.*<sup>38</sup> This system records simultaneously the extracellular voltage on the surface of the right atrium using 324 individual electrodes. The electrodes are 0.01 in. diameter silver wires embedded in a flexible substrate, called an electrode plaque, in a configuration shown in Fig. 1. The electrodes are chloridized before each use to minimize the noise they generate. The plaque is affixed to the epicardium of the right atrial free wall with sutures to the pericardium and the fatty tissue in the atrioventricular (AV) groove.

Extracellular electrograms are recorded from each electrode in the plaque with respect to a return electrode placed at the aortic root. The electrograms are band-pass filtered from 0.5 to 500 Hz, sampled at 2 kHz, and saved to disk. They are analyzed by differentiating the waveform using a five-point, Lagrange-polynomial-based algorithm<sup>39</sup> and displaying the resulting waveform on a computer as an array of elements corresponding to the geometry of the plaque. A computer program determines activation times for each plaque electrode using a level crossing routine. The activation detection process is illustrated in Fig. 2. Figure 2(A) shows the unprocessed extracellular electrogram and Fig. 2(B) shows the differentiated signal, which is compared to a threshold value [the solid horizontal line in Fig. 2(B)]. An activation is indicated by a threshold crossing only if the time interval to the previously detected activation is longer than 10 ms. The detected activations for the electrogram are

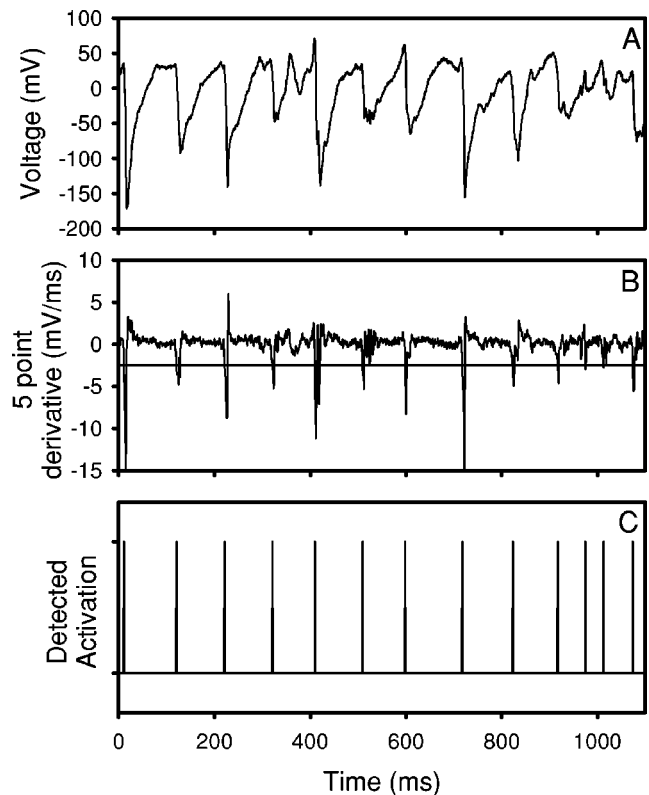


FIG. 2. The temporal evolution of the voltage recorded from (A) a single plaque electrode, (B) the five point derivative, and (C) detected activations.

shown as pulses in Fig. 2(C), where the inter-activation time intervals  $T_n$  correspond to the times between pulses.

The nonlinear dynamics feedback controller monitors only the electrode marked “recording electrode” in the figure. Feedback control is achieved by applying a cathodal stimulus current of 4 ms duration and amplitude in the range of 0.1–3.5 mA (chosen by the procedure described below) to the electrode marked “pacing electrode” in the figure. The return electrode is attached to a chest retractor that remains in place during the studies. The electrical stimulus is generated by a constant-current source whose timing is dictated by the control circuit described in Sec. V. We use different stimulus and recording electrodes because the constant-current pulse temporarily polarizes the stimulus electrode, thereby saturating the amplifiers and making observations of the temporal dynamics by this electrode impossible.

Before beginning an experimental run we first determine the amplitude of the stimulus current, which is accomplished using two different pacing protocols. The first protocol identifies the stimulus size needed to elicit a wave of activation. The second identifies the stimulus size that produces consistent paced dynamics. The first procedure involves pacing periodically (400–500 ms period) the right atrium via the stimulus electrode. The current of the pacing pulses is increased slowly until the dynamics of the whole right atrium are captured. This current amplitude is taken as the baseline level for the second protocol.

The second protocol identifies the minimum pacing current at which no further change in the window of bistability between 1:1 and 2:1 response patterns is detected, which we

believe is a convenient method for determining the current at which the strength-interval curve<sup>40</sup> begins to increase rapidly. Details of the procedure are given in Ref. 41, and the current determined using this approach is at least twice the amplitude determined using the first protocol.

The next step of the experiment is to induce atrial fibrillation in the nominally healthy sheep heart using three possible methods. We find that no single method is successful in inducing atrial fibrillation in a given animal and hence resort to a suite of techniques. We first attempt to induce fibrillation using the pacing protocol described above for measuring the bistability window. In 20% of the trials, atrial fibrillation is induced using this protocol.<sup>41</sup> When unsuccessful, the tissue is paced periodically with the period set to the shortest value at which a 1:1 response pattern behavior is observed (typically 130 ms). The periodic pacing is maintained for several minutes with the goal of increasing the excitability of the atrial tissue and inducing spatial variations in refractoriness.<sup>42</sup> Finally, if neither of these techniques establish fibrillation, we periodically pace the tissue at a fast rate (50 ms period) for several seconds (so-called “burst” pacing).

In experiments on five female  $63 \pm 5$  kg sheep, one of these pacing protocols successfully induced sustained atrial fibrillation or a fast organized macro-reentrant rhythm in two of the five animals. In two other animals, the pacing protocols only induced the fast organized macro-reentrant rhythm. In one of the five animals, no sustained complex spatio-temporal rhythm could be established using any of the pacing protocols.

#### IV. ATRIAL FIBRILLATION IN SHEEP

In this section we give examples of the different behaviors observed from a Lead II electrocardiogram and from the cardiac mapping system under conditions when no pacing stimuli are applied to the tissue while recording the dynamics. Figure 3(A) shows the ECG corresponding to normal sinus rhythm obtained by measuring the voltage differences between the left leg and right shoulder of the animal. It is important to note that this signal is a summation of the electrical activity of the whole heart, so it is not possible to distinguish the spatial patterning on the surface of the heart. The feature denoted by P is associated with excitation of the atria and the QRS feature corresponds to excitation in the ventricles. The feature labeled T is associated with the repolarization of the ventricle.

The spatio-temporal pattern of activation during normal sinus rhythm is shown in the series of panels in Figs. 3(B)–3(J). Each panel corresponds to a 4.5 ms time interval and the symbols indicate the spatial location of the electrodes. A black dot indicates the detection of an activation during the 4.5 ms interval and progressive panels show the observed activations in a sequence of equal time intervals. Arrows have been added to guide the eye through the time course of the wave. The wave of excitation originates at the sinus node (off the plaque in the upper left region) and propagates across the atrium. The wave of excitation shown in this figure corresponds to the “P-wave” part of cardiac cycle and

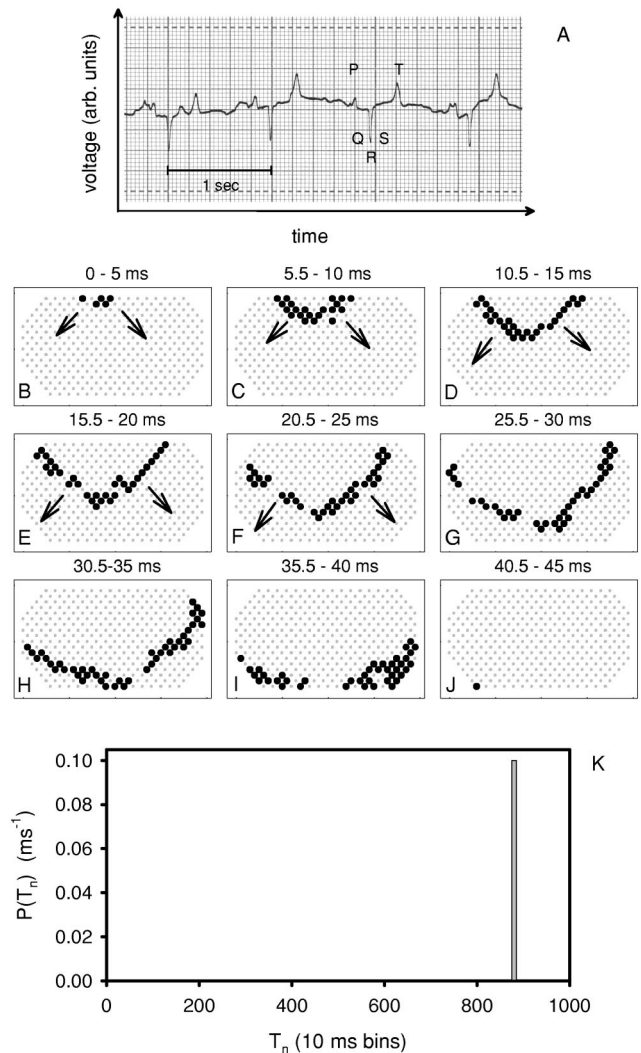


FIG. 3. Normal sinus rhythm. (A) A Lead II electro-cardiogram of normal sinus rhythm. The deflection of the trace corresponds to the phases of a heart beat. The P complex corresponds to the depolarization of the atria. The QRS complex part of the signal corresponds to ventricular depolarization, and the T-wave is the repolarization of the ventricles. (B)–(J) A temporal sequence of normal sinus rhythm in a right sheep atrium measured with the cardiac mapping system. The wave originates in the sinus node (off plaque at the top to the left of the middle of the diagram) and propagates across the atrium. Each of the panels represents a 4.5 ms time interval. The black dots show the location of the leading edge of activation during that time interval of each panel. The plaque is approximately  $7.0 \text{ cm} \times 3.2 \text{ cm}$  and the wave of excitation travels across it in 31 ms. This pattern repeats approximately once per second. (K) Experimental probability distribution of inter-activation time intervals during normal sinus rhythm detected from 100 electrodes from the center of the plaque attached to the right atrium during a recording time of 2 s (encompassing two heart beats). The bin sizes are 10 ms. Note that all points fall in a single bin centered at 880 ms even though the distribution categorizes inter-activation intervals observed at many different locations on the atrium.

repeats approximately once per second. The total propagation time across the plaque (33 mm width) is about 31 ms.

To quantify the observed behavior, we calculate a probability density  $P(T_n)$ , where  $P(T_n)\Delta T_n$  represents approximately the probability that a measured inter-activation interval will fall between  $T_n$  and  $T_n + \Delta T_n$  in the limit as  $\Delta T_n$  becomes small. The density  $P(T_n)$  is determined by con-

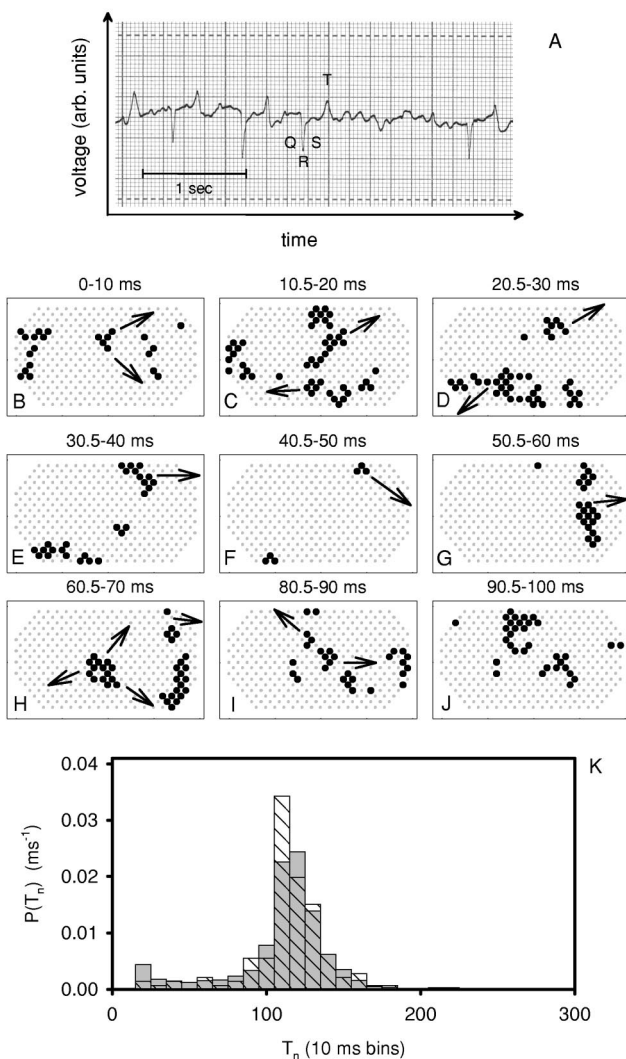


FIG. 4. Atrial fibrillation. (A) A Lead II electro-cardiogram during atrial fibrillation. There is no longer a clear PQRST complex, the waveform is seemingly random, and the ventricle is firing at a more normal, slower rate. (B)–(J) A series of panels showing the temporal evolution of atrial fibrillation. (K) Experimental probability distribution of inter-activation intervals observed during atrial fibrillation. The solid gray bars are the distribution from the 100 middle electrodes. The diagonal-line bars are the distribution from the “recording electrode.” Note the large width of the distribution in comparison to normal sinus rhythm.

structuring a histogram of the inter-activation intervals, scaled to the total number of points and the bin width of the histogram. The probability density is determined from data collected from the 100 electrodes closest to the center of the plaque during the entire 15 s recording period (encompassing ~1500 inter-activation intervals). As seen in Fig. 3(K),  $P(T_n)$  corresponding to normal sinus rhythm during one experimental recording consists of a single 10-ms-wide bin centered at 880 ms.

This coordinated behavior can give way to a complex, fast rhythm known as fibrillation. Figure 4(A) shows the ECG during fibrillation where it is seen that there is no clear P-wave and the QRS complex arrives at seemingly random intervals. In addition, there is no time when activity ceases on the heart. The corresponding activation wave recorded by the mapping system is shown in Figs. 4(B)–4(J). Since we

observe that the propagation speed is slower during atrial fibrillation (consistent with previous observations<sup>43</sup>), each panel corresponds to a 9.5 ms time interval rather than the 4.5 ms interval used in Figs. 3(B)–3(J). It is seen that the waves of activation do not follow any clear pattern. At several instances (panels B and I), waves break into two, or appear to emanate near the center of the plaque (panel H), likely originating from electrical activity propagating through the subendocardial muscle network.<sup>44</sup> At other times (not shown), two waves collide and annihilate each other. Note that some portions of the muscle contract frequently during fibrillation, which contrasts normal sinus rhythm where a contraction occurs about once per second. During atrial fibrillation there is no single point of origin for the excitation, the observed activity is self-sustaining, the shape of the wavefront is uneven, and its speed varies widely from location to location. Figure 4(K) shows  $P(T_n)$  from the single “recording electrode” (stripes) and the 100 central electrodes (solid gray) during atrial fibrillation. It is seen that the average rate is much faster, there is a large variance in  $T_n$ , and that the local dynamics are similar to the dynamics over the entire right atrium.

We also frequently observe a fast organized macro-reentrant rhythm that is reminiscent of a behavior known at atrial flutter. Figure 5(A) shows the ECG during this behavior and the spatial-temporal distribution is shown in Figs. 5(B)–5(J). It is seen that a well organized wave pattern crosses the surface of the atrium. This structure usually recurs in a similar form with a period of a few hundred milliseconds and it does not originate from the sinus node. It occasionally breaks up into fibrillation or shifts back-and-forth between the macro-reentrant rhythm and fibrillation. Figure 5(K) shows the single and multipoint probability density of the inter-activation intervals, where it is seen that both distributions cluster around 110 ms. In addition, the variance of the intervals is approximately the same for both distributions, indicating that similar dynamics occur everywhere on the atria. Notice that the average inter-activation interval is much shorter than that observed for normal sinus rhythm (Fig. 3).

## V. CONTROL AND ACTUATION

The goal of our nonlinear-dynamics-based closed-loop feedback protocol is to stabilize a periodic rhythm, characterized by an inter-activation time  $T^*$ , that is embedded in the dynamics characteristic of fibrillation for which the inter-activation time sequence  $T_n$  follows a complex pattern (see Fig. 2). It attempts to achieve this goal by pacing occasionally the cardiac muscle with small shocks at a single spatial location. When successful,  $T_n = T^*$  for all  $n$  and paces are only applied when the controller senses that the dynamics are beginning to depart from the desired periodic rhythm. The shock timing is adjusted in real time using a control algorithm we call projective time delay autosynchronization (PTDAS) because it attempts to synchronize the most recently measured inter-activation interval  $T_n$  with the previous interval  $T_{n-1}$  by inducing an activation at a time projected by the algorithm. The scheme is “single-sided” in that

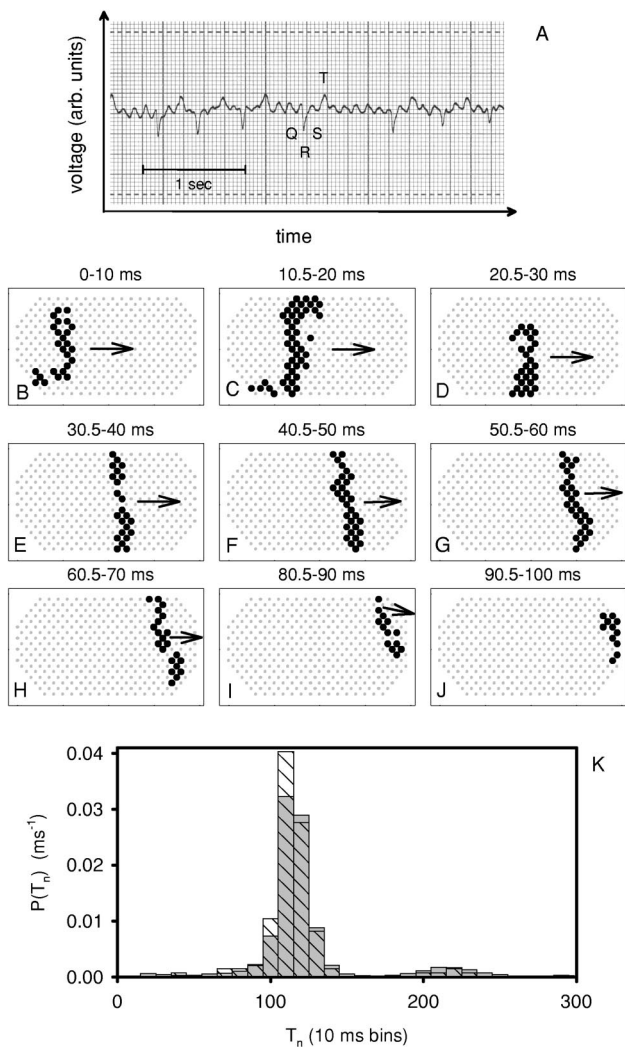


FIG. 5. Fast organized macro-reentrant rhythm. (A) A Lead II electrocardiogram during an organized macro-reentrant rhythm that circulated from the right to the left atrial chambers and back to the right in a cyclic pattern. It is seen that the atrial chambers are firing in a more periodic manner in comparison to atrial fibrillation but the atrial rhythm is fast. (B)–(J) A series of panels showing an organized wave of excitation traveling across the right atrium and then to the left atrium in a large reentrant circuit. (K) Experimental probability distribution of the inter-activation intervals observed during the macro-reentrant rhythm. The solid gray bars are the distribution from the 100 middle electrodes. The diagonal-line bars are the distribution from the “recording electrode.” Notice that the spread in the distribution is similar to that observed for atrial fibrillation shown in Fig. 4(K).

it can only shorten the inter-activation time but not lengthen it. In the situation where an activation does not occur within the time calculated by the controller, it stimulates the tissue at the projected time in an attempt to induce an activation. If a naturally occurring activation is detected at or before the projected time, the controller does nothing. The strength of the stimulus is not adjusted during the experiment and is set the value determined using the method described in Sec. III. The feedback protocol is based on a scheme developed for controlling fast, potentially nonstationary, physical systems.<sup>31</sup>

The PT DAS controller compares consecutive inter-activation intervals to generate an error signal given by

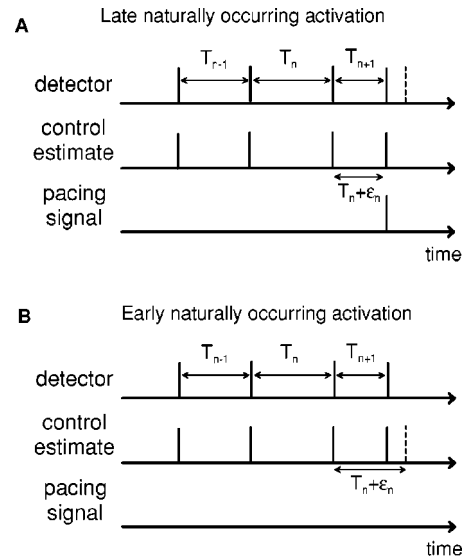


FIG. 6. Illustration of the control sequence when (A) the next naturally occurring activation happens after the control stimulus is applied, and (B) when it arrives before the time the stimulus should be applied.

$$\epsilon_n = -\gamma(T_n - T_{n-1}), \tag{1}$$

where  $\gamma$  is the controller gain. To guide the system to the desired periodic pattern with inter-activation interval  $T^*$ , the next activation should occur at a time

$$T'_{n+1} = T^* + \epsilon_n. \tag{2}$$

However, since we do not know  $T^*$  a priori, we estimate  $T^*$  by  $T_n$  and attempt to force an activation at a time

$$\tilde{T}_{n+1} = T_n + \epsilon_n. \tag{3}$$

If the next natural (not paced) activation interval is a time longer than  $\tilde{T}_{n+1}$ , the controller stimulates the tissue at time  $\tilde{T}_{n+1}$  since the previously detected activation, as illustrated in Fig. 6(A). If  $T_{n+1} \leq \tilde{T}_{n+1}$ , no stimulus is applied and the controller is reset, as illustrated in Fig. 6(B). Since we do not have a detailed model for predicting the proper value of the feedback gain  $\gamma$ , we perform many experimental trials for different values of  $\gamma$ . Based on previous results,<sup>29,45</sup> we expect it should be in the range  $0 < \gamma < 2$ . As discussed below, feedback gains in this range have little effect on the dynamics so we also explore the range  $-2 < \gamma < 0$  for completeness. Note that inherent to the controller design is the assumption that the applied stimulus induces an activation. Adaptive estimation routines<sup>25</sup> are now available for determining  $\gamma$  whose application requires that the dynamics be within a neighborhood of the desired unstable period orbit. Based on our observation described below, the dynamics did not appear to visit such a neighborhood for an extended period and hence these estimation schemes may not be applicable. Additional experiments are needed to address this point.

We have found that the control algorithm can possibly lead to a condition of “latch-up” where it paces the tissue as rapidly as possible (at the limit of the speed of the controller) if the sign of the controller is chosen incorrectly or if the desired unstable periodic orbit is not of the flip-saddle type.

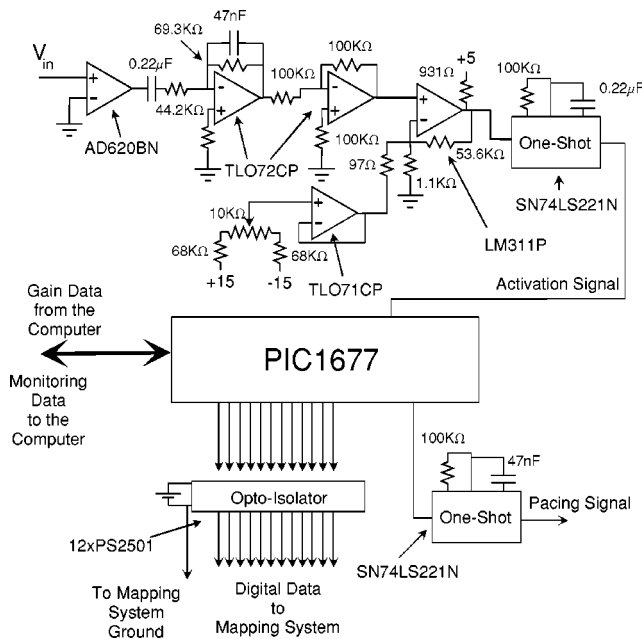


FIG. 7. A schematic of the PIC1677-based PT DAS controller. The signal from the “recording electrode” is filtered and a threshold detector is employed to indicate activations. A threshold crossing causes a pulse to be sent to the microcontroller, which implements the PT DAS algorithm. The microcontroller generates pulses that are sent to a constant current source to stimulate the tissue via the pacing electrode, as well as generating diagnostic data.

One solution to this problem is to require the controller to turn off occasionally and let the system evolve naturally.<sup>46</sup> This requirement is met by preventing the controller from pacing the tissue two times in a row, so at least every other activation the system evolves according to its natural dynamics. The added benefit of occasional application of perturbations is that the dynamics can be observed in the absence of control,<sup>25</sup> thereby preventing the obscuration of an activation by the stimulus artifact.

The PT DAS scheme is implemented using an analog circuit to detect activations and a microcontroller to calculate the timing of the control pulse. A schematic of the control circuit is shown in Fig. 7. The voltage from a single electrode is band-pass filtered to generate approximately the derivative of the signal and to reduce noise in the signal.<sup>47</sup> The filtered signal is compared to a manually set threshold and a threshold crossing causes a pulse to be sent to the microcontroller. By a visual inspection, we verified that this circuit properly detected activations.

A PIC1677 microcontroller from MicroChip generates the feedback stimulus that is applied to the tissue based on the algorithm described above. The time between activations is calculated with a timer built into the microcontroller, which is stored on a stack for use in calculating the timing of the output pulse. The gain for the control algorithm is supplied by a personal computer. The microcontroller generates a control pulse that is sent to the constant-current source which in turn delivers the stimulus to the “pacing electrode.”

## VI. RESULTS

The possible outcomes of our experiments on control of *in vivo* atrial fibrillation can be categorized in three groups.

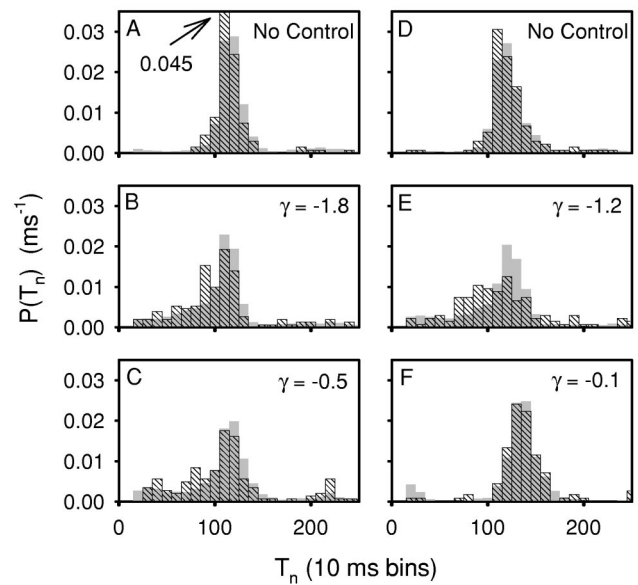


FIG. 8. Experimental probability distributions for negative feedback gains using the PT DAS scheme during atrial fibrillation. The solid gray bars are the distribution from the 100 middle electrodes. The diagonal-line bars are the distribution from the eight electrodes closest to the control site.

The controller might suppress fibrillation everywhere within the atrium and all inter-activation time intervals are equal  $T^*$  at every spatial location. Another scenario is successful control near the control site with inter-activation intervals equal to  $T^*$  in this region but entrainment is lost at large distances. To distinguish between these two situations, we compute normalized inter-activation time-interval histograms for the eight electrodes adjacent to the recording and pacing intervals and compare them to the histogram for the closest 100 electrodes. The final scenario is that there is no effect of the control on the dynamics.

Our experimental results using PT DAS are inconclusive at this preliminary stage. In 40 trials with each of the two animals that showed fibrillation, we find that the controller does not regularize the dynamics for any value of  $\gamma$  for the range explored ( $\gamma = -2$  to  $2$  in increments of  $0.1$ ). Experimental trials with feedback control applied are interspersed with recordings when control is turned off to monitor the underlying dynamics. While we do not observe a regularization of the  $T_n$ 's, we observe a difference in the local and global dynamics in one trial when control is actuated [see Fig. 8(E)], and we also observe a noticeable decrease in the mean value of  $T_n$  in another trial [see Fig. 8(F)].

Since we do not observe significant regularization of the cardiac dynamics when control is actuated, we present data as inter-activation time-interval probability distributions from only a few trials to illustrate the range of observed behaviors, as shown in Figs. 8 and 9. Each figure contains six panels showing a set of probability densities for a set of PT DAS experiments with several different feedback gains. The panels in a vertical column are collected in sequence, where the first panel (with no control) is collected first so that differences between the presence and absence of control can be discerned readily. The data cover both negative (Fig. 8) and positive (Fig. 9) values. The gray bars in each distri-

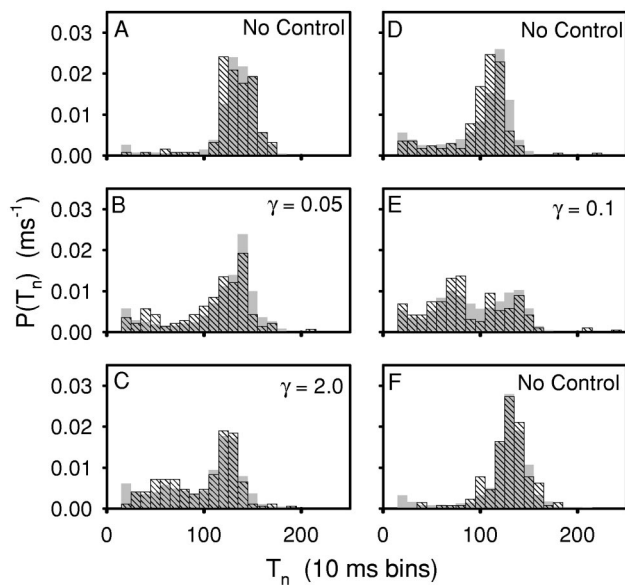


FIG. 9. Experimental probability distributions for positive feedback gains using the PTDas scheme during atrial fibrillation. The solid gray bars are the distribution from the 100 middle electrodes. The diagonal-line bars are the distribution from the eight electrodes closest to the control site.

bution are for 100 electrodes from the center of the plaque. The diagonal striped lines are from the controller's "recording electrode" and nearest-neighbor electrodes.

As can be seen in the figures, the distributions for the adjacent electrodes are similar to that seen in the spatially broader 100-point measure of the atrial activity, except for the single trial shown in Fig. 8(E), implying that control of even the local dynamics does not occur in most situations. Sequence Figs. 8(D)–8(F) is also of interest because there is a substantial shift in the mean inter-activation time: from 124 ms with no control to 146 ms with  $\gamma = -0.1$ . While a noticeable decrease, it may be due to changes in the tissue properties rather than the effects of control, as discussed below.

In many cases, it is observed that control actually increases the variance in  $T_n$ . An extreme situation shown in Fig. 9(E) for  $\gamma = 0.1$  where the mean value of  $T_n$  drops to 88 ms and the variance increased to 44 ms in comparison to the preceding case of no control (mean 146 ms, variance 31 ms) shown in Fig. 9(D). Surprisingly, we observe that the dynamics shift back to a narrow distribution (variance 23 ms) but with a longer mean inter-activation time (128 ms) soon after control is turned off, as shown in Fig. 9(F). This rate slowdown after control is switched off may be due to the fact that restitution properties of the muscle change<sup>42</sup> during the episode of rapid activations shown in Fig. 9(E) caused by the effects of the controller. Note that the shift in the mean  $T_n$  from Figs. 9(D)–9(F) is comparable to that seen between Figs. 8(D)–8(E), putting into question the significance of the result shown in Fig. 8(E).

## VII. DISCUSSION AND OUTLOOK

The results of our preliminary experiments are somewhat surprising in light of the previous experiments of Ditto

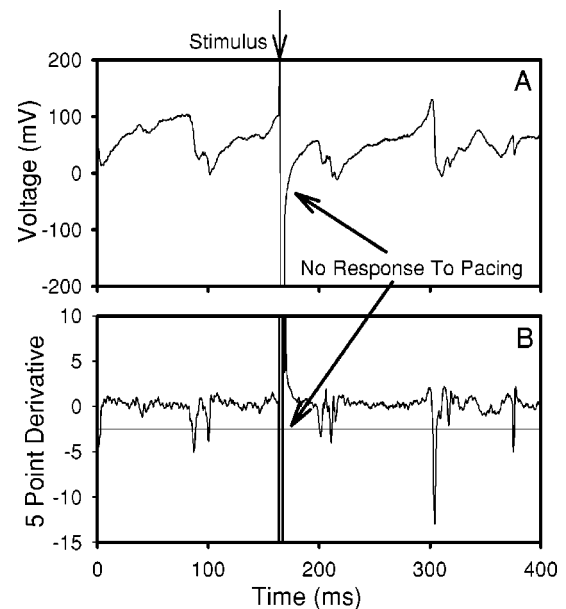


FIG. 10. The temporal evolution of the (A) voltage and (B) derivative of the voltage obtained from the "recording electrode" during atrial fibrillation capturing the moment when a control stimulus is applied to the tissue.

*et al.*<sup>19</sup> where they observed that they could regularize the spatially localized inter-activation dynamics of *in vivo* human atrial fibrillation using a similar closed-loop feedback method. While the procedures are similar, there are many differences in the two experiments: The PTDas control scheme is different than the PPF method in that a comparison is made between the current and past interbeat intervals (PTDas protocol) rather than the difference between the current interbeat interval and a value that is determined during a "learning phase" before control is initiated (PPF protocol). Additional differences in the experiments are that sheep atrial tissue is different from human, the sheep are nominally healthy whereas the human patients suffered from chronic atrial fibrillation (which is known to change cardiac tissue properties), we performed the experiment on the epicardium whereas Ditto *et al.* used the endocardium, and we explored only a finite number of feedback gains over a limited range whereas they chose the gain based on an analysis of the inter-activation intervals during a "learning phase" of their experiment. Hence, we can only state that our control scheme did not achieve results as noticeable as their technique.

Going one step further, we suggest one possible reason for the ineffectiveness of the PTDas controller. We observe that every stimulus delivered to the tissue does not induce an activation, a key assumption of our control protocol. For example, Fig. 10 shows a time series when control is actuated and the applied stimulus does not induce an activation, as can be seen in Fig. 10(B) where an activation is not detected by our circuitry immediately following the applied stimulus. A possible explanation for why some paces are ignored is that the stimulus occurs while the tissue is still refractory from the previous action potential.

While our experiments are not as successful as hoped originally, they provide new insights into the fundamental

mechanisms that regulate the dynamics of cardiac muscle subjected to small, appropriately timed electrical stimuli. We have attempted to explain carefully our experimental procedures so as to help guide the refinement of nonlinear dynamics control techniques for stabilizing cardiac arrhythmias.

## ACKNOWLEDGMENTS

We gratefully acknowledge invaluable collaborations with Henry Greenside, Wanda Krassowska, David Schaeffer, and Joshua Socolar. This work was supported in part by the Whitaker Foundation and the National Institute of Health (NIH) under Grant No. HL-64238.

- <sup>1</sup>L. Glass, *Phys. Today* **49** (8), 40 (1996).
- <sup>2</sup>For a recent review, see A.T. Winfree, *Chaos* **8**, 1 (1998) and the accompanying articles on the special Focus Issue on *Fibrillation in Normal Ventricular Myocardium*.
- <sup>3</sup>C.J. Wiggers, *Am. Heart J.* **20**, 399 (1940).
- <sup>4</sup>D.P. Zipes, J. Fischer, R.M. King, A. Nicoll, and W.W. Jolly, *Am. J. Cardiol.* **36**, 37 (1975).
- <sup>5</sup>R.E. Ideker, P.-S. Chen, N. Shibata, P.G. Colavita, and J.M. Wharton, in *Non-Pharmacological Therapy of Tachyarrhythmias*, edited by G. Breithardt, M. Borggrefe, and D. Zipes (Futura, Mount Kisco, 1987), pp. 449–464.
- <sup>6</sup>E. Ott, C. Grebogi, and J.A. Yorke, *Phys. Rev. Lett.* **64**, 1196 (1990).
- <sup>7</sup>T. Shinbrot, C. Grebogi, E. Ott, and J.A. Yorke, *Nature (London)* **363**, 411 (1993).
- <sup>8</sup>E. Ott and M. Spano, *Phys. Today* **48** (5), 34 (1995).
- <sup>9</sup>A. Garfinkel, M.L. Spano, W.L. Ditto, and J.N. Weiss, *Science* **257**, 1230 (1992).
- <sup>10</sup>K. Hall, D. J. Christini, M. Tremblay, J. J. Collins, L. Glass, and J. Billette, *Phys. Rev. Lett.* **78**, 4518 (1997).
- <sup>11</sup>D.J. Christini, K. Hall, J.J. Collins, and L. Glass, in *Handbook of Biological Physics, Volume 4: Neuro-Informatics, Neural Modeling*, edited by F. Moss and S. Gielen (Elsevier, New York, 2001), p. 205.
- <sup>12</sup>D.J. Christini, K.M. Stein, S.M. Markowitz, S. Mittal, D.J. Slotwiner, M.A. Scheiner, S. Iwai, and B.B. Lerman, *Proc. Natl. Acad. Sci. U.S.A.* **98**, 5827 (2001).
- <sup>13</sup>D.J. Gauthier, S. Bahar, and G.M. Hall, in *Handbook of Biological Physics, Volume 4: Neuro-informatics, Neural Modelling*, edited by F. Moss and S. Gielen (Elsevier, Amsterdam, 2001), p. 229.
- <sup>14</sup>G.M. Hall and D.J. Gauthier, *Phys. Rev. Lett.* **88**, 198102 (2002).
- <sup>15</sup>R.A. Gray, A.M. Pertsov, and J. Jalife, *Nature (London)* **392**, 75 (1998).
- <sup>16</sup>F.X. Witkowski, L.J. Penkoske, P.A. Giles, W.R. Spano, M.L. Ditto, and A.T. Winfree, *Nature (London)* **392**, 78 (1998).
- <sup>17</sup>M.C. Cross and P.C. Hohenberg, *Science* **263**, 146 (1994).
- <sup>18</sup>W.-J. Rappel, F. Fenton, and A. Karma, *Phys. Rev. Lett.* **83**, 456 (1999).
- <sup>19</sup>W.L. Ditto, M.L. Spano, V. In, J. Neff, B. Meadows, J.J. Langberg, A. Bolmann, and K. McTeague, *Int. J. Bifurcation Chaos Appl. Sci. Eng.* **10**, 593 (2000).
- <sup>20</sup>P.-S. Chen, P.D. Wolf, E.G. Dixon, N.D. Danieley, D.W. Frazier, W.M. Smith, and R.E. Ideker, *Circ. Res.* **62**, 1191 (1988).
- <sup>21</sup>C. Kirchhof, F. Chorro, G.J. Scheffer, J. Brugada, K. Konings, Z. Zetelaki, and M. Allesie, *Circulation* **88**, 736 (1993).
- <sup>22</sup>B.H. KenKnight, P.V. Bayly, R.J. Gerstle, D.L. Rollins, P.D. Wolf, W.M. Smith, and R.E. Ideker, *Circ. Res.* **77**, 849 (1995).
- <sup>23</sup>M. Watanabe and R. F. Gilmour, Jr., *J. Math. Biol.* **35**, 73 (1996).
- <sup>24</sup>D.J. Christini and J.J. Collins, *Phys. Rev. E* **53**, R49 (1996).
- <sup>25</sup>D.J. Christini and D.T. Kaplan, *Phys. Rev. E* **61**, 5149 (2000).
- <sup>26</sup>S.J. Schiff, K. Jerger, D.H. Duong, T. Chang, M.L. Spano, and W.L. Ditto, *Nature (London)* **370**, 615 (1994).
- <sup>27</sup>D. Pierson and F. Moss, *Phys. Rev. Lett.* **75**, 2124 (1995).
- <sup>28</sup>D.J. Christini and J.J. Collins, *Phys. Rev. Lett.* **75**, 2782 (1995).
- <sup>29</sup>D.J. Gauthier and J.E.S. Socolar, *Phys. Rev. Lett.* **79**, 4938 (1997).
- <sup>30</sup>K. Hall and D.J. Christini, *Phys. Rev. E* **63**, 046204 (2001).
- <sup>31</sup>D.W. Sukow, M.E. Bleich, D.J. Gauthier, and J.E.S. Socolar, *Chaos* **7**, 560 (1997).
- <sup>32</sup>L. Glass and M. F. Josephson, *Phys. Rev. Lett.* **75**, 2059 (1995).
- <sup>33</sup>V.N. Biktashev and A.V. Holden, *Proc. R. Soc. London, Ser. B* **261**, 211 (1995).
- <sup>34</sup>I. Aranson, H. Levine, and L. Tsimring, *Phys. Rev. Lett.* **72**, 2561 (1994).
- <sup>35</sup>G.V. Osipov, B.V. Shulgin, and J.J. Collins, *Phys. Rev. E* **58**, 6955 (1998).
- <sup>36</sup>G.V. Osipov and J.J. Collins, *Phys. Rev. E* **60**, 54 (1999).
- <sup>37</sup>S. Sinha, A. Pande, and R. Pandit, *Phys. Rev. Lett.* **86**, 3678 (2001).
- <sup>38</sup>R.E. Ideker, W.M. Smith, P.D. Wolf, N.D. Danieley, and F.R. Bartram, *PACE* **10**, 281 (1987).
- <sup>39</sup>R.L. Burden, J.D. Faires, and A.C. Reynolds, *Numerical Analysis* (Prindle, Weber & Schmidt, Boston, MA, 1978), p. 179.
- <sup>40</sup>D.R. Chialvo, D.C. Michaels, and J. Jalife, *Circ. Res.* **66**, 525 (1990).
- <sup>41</sup>R.A. Oliver, G.M. Hall, S. Bahar, W. Krassowska, P.D. Wolf, W. Krassowska, E.G. Dixon-Tulloch, and D.J. Gauthier, *J. Cardiovasc. Electrophysiol.* **11**, 797 (2000).
- <sup>42</sup>V. Elharrar and B. Surawicz, *Am. J. Physiol. (Heart Circ. Physiol. 13)* **244**, H782 (1983).
- <sup>43</sup>M.A. Allesie, K. Konings, C.J.H.J. Kirchhof, and M. Wijffels, *Am. J. Cardiol.* **77**, 10A (1996).
- <sup>44</sup>R.A. Gray, A.M. Pertsov, and J. Jalife, *Circulation* **94**, 2649 (1996).
- <sup>45</sup>J.E.S. Socolar and D.J. Gauthier, *Phys. Rev. E* **75**, 6589 (1998).
- <sup>46</sup>P. Cheruvu and J.E.S. Socolar, private communication.
- <sup>47</sup>D.M. Beams, in *Design of Cardiac Pacemakers*, edited by J.G. Webster (IEEE, Piscataway, NJ, 1995), Chap. 8.